Inorg. Chem. **2008**, *47*, 7302−7308

Synthesis and Characterization of Phase-Pure Manganese(II) and Manganese(III) Silicalite-2

Adrian Lita,[†] Xisai Ma,[†] Robert W. Meulenberg,[‡] Tony van Buuren,[‡] and A. E. Stiegman*[,†]

Department of Chemistry and Biochemistry, Florida State University, Tallahassee, Florida 32306, and The Materials Science & Technology Division, Lawrence Livermore National Laboratory, P.O. Box 808, L-371, Livermore, California 94550

Received February 26, 2008

Manganese silicalite-2 was synthesized at high pH using the molecular cluster $Mn_{12}O_{12}(O_2CCH_3)_{16}$ as a Mn source. The silicalite-2 (ZSM-11) materials were synthesized using 3,5-dimethyl-*N*,*N*-diethylpiperdinium hydroxide as a structure-directing agent to produce phase-pure ZSM-11 materials. No precipitation of manganese hydroxide was observed, and synthesis resulted in the incorporation of up to 2.5 mol % Mn into the silicalite-2 with direct substitution into the framework verified by the linear relationship between the unit cell volume and loading. The Mn is reduced to Mn^{II} during hydrothermal synthesis and incorporated into the silicalite-2 framework during calcination at 500 °C. Further calcination at 750 °C does not affect the crystallinity but oxidizes essentially all of the Mn^{II} to Mn^{III} in the framework. The large difference in oxidation temperatures between the II and III oxidation states provides a means of producing relatively pure manganese(II) and manganese(III) silicalite-2 materials for applications such as catalysis.

Introduction

Molecular-sieve materials in which transition-metal ions have been substituted into a silicate or aluminosilicate framework have been of considerable interest because of their potential as selective heterogeneous oxidation catalysts. Among the most notable and commercially useful of these is titanium silicalite-1 (TS-1), which catalyzes the hydroxylation of phenol using hydrogen peroxide. In the case of TS-1, the high catalytic activity arises from the isomorphic substitution of Ti^{IV} for Si^{IV} in the silicalite lattice.[1] Taking TS-1 as a paradigm, other metal ions possessing similar ionic radii have been substituted into the silicalite framework and explored for catalytic activity. Among transition metals, manganese is a particularly attractive candidate for incorporation because of its established activity as both homogeneous and heterogeneous catalysts in other ligand environments.[2–4]

An inherent difficulty with transition-metal substitution into silicalite, and one that is acute with Mn, is that the basic conditions typically utilized to produce high-quality materials cause precipitation of the metal as the hydroxide. While different strategies have been used to overcome this problem, none have generated high-quality Mn-substituted silicalite with levels of metal incorporation comparable to those attained with Ti. We report here the use of the Mn cluster complex, $Mn_{12}O_{12}(O_2CCH_3)_{16}$, to deliver Mn ions into a silicalite-2 (ZSM-11) lattice under basic conditions. Manganese silicalite-2 (ZSM-11) materials were synthesized using 3,5-dimethyl-*N*,*N*-diethylpiperidinium (DDP) as the structure-directing agent (SDA). This produced phase-pure manganese silicalite-2 of high crystallinity with Mn substitution in amounts up to 2.5 mol % achieved. This is, to the best of our knowledge, the highest and most systematic incorporation of manganese into a silicalite.

Experimental Section

Synthesis. $Mn_{12}O_{12}(O_2CCH_3)_{16}$ and 3,5-dimethyl-*N*,*N*-diethylpiperidinium hydroxide were synthesized by published procedures.[5,6] In a typical preparation, 24.405 mL of a 0.7895 M 3,5-dimethyl-

* To whom correspondence should be addressed. E-mail: stiegman@chem.fsu.edu.
† Florida State University.
‡ Lawrence Livermore National Laboratory.

(1) Notari, B. *Catal. Today* **1993**, *18*, 163.
(2) Cao, H.; Suib, S. L. *J. Am. Chem. Soc.* **1994**, *116*, 5334.
(3) Fabrizioli, P.; Burgi, T.; Baiker, A. *J. Catal.* **2002**, *207*, 88.
(4) Son, Y. C.; Makwana, V. D.; Howell, A. R.; Suib, S. L. *Angew. Chem., Int. Ed.* **2001**, *40*, 4280.
(5) Lis, T. *Acta Crystallogr., Sect. B: Struct. Commun.* **1980**, *36*, 2042.
(6) Nakawaga, Y. U.S. Patent 5,645,812, 1997.

10.1021/ic800366j CCC: $40.75
Published on Web 07/12/2008

N,*N*-diethylpiperidinium hydroxide solution was placed in a three-necked flask equipped with a magnetic stirrer under a N_2 flow. A total of 15.167 mL of freshly distilled tetraethyl orthosilicate (TEOS; Aldrich, 98%) was added over a period of 30 min under constant stirring. After 1 h, 0.117 g of $Mn_{12}O_{12}(O_2CCH_3)_{16}$ in 5 mL of methanol was added. The solution was stirred under N_2 for a period of 1 h, after which 10 mL of nanopure water (18.0 Ω^{-1}; Barnsted E-Pure system) was added slowly. The solution was stirred overnight, after which the flask was heated to 78 °C for 1.5 h, resulting in evaporation of some of the solvent. The clear solution obtained was transferred into a Teflon-lined bomb of 250 cm^3 capacity and placed in an oven at 114 °C for 3 days followed by heating at 175 °C for an additional 4 days. The solid was recovered by centrifugation followed by filtration. The filtrate was washed thoroughly with nanopure water, dried at 120 °C in air for 24 h, and calcined at 500 °C in air for 48 h.

X-ray Fluorescence. The weight percent of manganese in the silicalite-2 materials was quantified using an Oxford Instruments ED 2000 X-ray fluorescence instrument. For quantitative determination, the instrument was calibrated against reference standards of known concentration of Mn doped into silica gel.

X-ray Diffraction (XRD). Powder XRD patterns were collected on a Siemens D500 diffractometer (40 kV, 30 mA, $2\theta = 2°$ min^{-1}) using Cu Kα radiation. The samples were ground to a grain size of 5−10 μm using a mortar and pestle and then mounted on a glass slide using the smear mounting method.

Electron Paramagnetic Resonance (EPR). EPR spectroscopy spectra were obtained on a Bruker E-500 spectrometer operating at X and Q band. The *g* values of the samples were obtained with reference to a standard diphenylpicrylhydrazyl resonance at $g = 2.0036$.

Soft X-ray Absorption Near-Edge Spectroscopy (XANES). XANES spectra were acquired at the undulator Beamline 8.0.1 at the Advanced Light Source at the Lawrence Berkeley National Laboratory. The standards and unknown samples were pressed into carbon tape, and the spectra were taken on these powder samples. XANES experiments were conducted using the total electron yield detection method, where the total photocurrent is measured as the photon energy is scanned through the absorption edges. The experimental energy resolution was ~0.10 eV at the Mn $L_{2,3}$ edge. The incident photon flux was measured with a highly transmissive gold grid, and all spectra were normalized to the current from the gold grid. All spectra were recorded at room temperature and base pressures of less than 5×10^{-9} Torr.

Gas Physisorption Measurement. Nitrogen adsorption−desorption measurements were performed at 77 K on a Micrometrics ASAP 2020 sorptometer. Prior to measurement, all samples, previously dried at 500 and 750 °C, were degassed for 1 h at 90 °C followed by 4 h at 350 °C. Adsorption and desorption isotherms over a range of relative pressure ($P/P°$) of 0.01−0.95 were collected for all samples. Surface areas were determined from the Brunauer−Emmett−Teller (BET) equation in a relative pressure range between 0.01 and 0.10.[7] Micropore volumes and the average pore size were determined using the method of Horvath−Kawazoe.[8] All isotherms are described using IUPAC nomenclature.[9]

Results and Discussion

The incorporation of manganese into silicalite under the high-pH conditions needed to produce materials of high crystalline quality is difficult because of the ready formation and poor solubility of manganese hydroxide. For example, for Mn^{II} ions, which are common reagents, the hydroxide has a K_{sp} of $\sim 10^{-13}$.[10] Previous reports of manganese silicalite synthesis have sought to avoid this problem in different ways. In the earliest report, the reaction was carried out at low pH using fluoride as a mineralizing agent.[11] In that work, infrared spectroscopic evidence indicated that substitution into the framework had been achieved; however, the amount of manganese incorporated was small. In later studies, Mn^{2+} ions were exchanged into the layered silicate sodium magadiite, which was then hydrothermally treated to form the silicalite-1 MFI structure.[12] Recently, manganese silicalite-1 has been synthesized under basic conditions using manganese acetate as the metal ion source.[13] This process succeeded in incorporating Mn ions into the lattice; however, the material produced was biphasic and the amount of manganese incorporated was low.

Manganese silicalite-2 was synthesized under standard conditions for silicalite-2 using 3,5-dimethyl-*N*,*N*-diethylpiperidinium hydroxide as the SDA. The manganese acetate cluster complex, $Mn_{12}O_{12}(O_2CCH_3)_{16}$, was added in a methanol solution, with the amount added being determined by the amount of manganese desired in the silicalite product. The resulting solid was transparent even after addition of the base, indicating that precipitation of manganese as the hydroxide was not occurring. The solution was placed in a Teflon-lined bomb, and hydrothermal synthesis was carried out. After synthesis, a white, uniform microcrystalline powder was recovered from the colorless clear mother liquor by centrifugation followed by filtration. Calcination to remove the template at 500 °C for 24 h under oxygen resulted in a gray powder.

Nitrogen physisorption of the powder gave a type I isotherm with a type H4 hysteresis loop characteristic of microporosity and typical of the isotherms observed for silicalites.[9,14] The BET surface area is 278.7 m^2/g, and the median pore width is 0.45 nm. Powder XRD of calcined (500 °C) 1 mol % manganese silicalite-2 powder gave a well-resolved diffraction pattern with sharp reflections suggestive of well-formed crystallites (Figure 1a). Analysis of the pattern showed it to be phase-pure ZSM-11, as was expected from this SDA, which is confirmed by the observation of diffraction peaks at $2\theta = 6.2°$ and 18.7° associated with the 110 and 330 reflections, which are allowed for ZSM-11 (MEL) but not ZSM-5 (MFI). In addition, two sharp intense

(7) Brunauer, S.; Emmett, P. H.; Teller, E. *J. Am. Chem. Soc.* **1938**, *60*, 309.
(8) Horvath, G.; Kawazoe, K. *J. Chem. Eng. Jpn.* **1983**, *16*, 470.
(9) Sing, K. S. W.; Everett, D. H.; Haul, R. A. W.; Moscou, L.; Pierotti, R. A.; Rouquerol, J.; Siemieniewska, T. *Pure Appl. Chem.* **1985**, *57*, 603.
(10) Peters, D. G.; Hayes, J. M.; Hieftje, G. M. *Chemical Separations and Measurements*, 1st ed.; W. B. Saunders: Philidelphia, 1974.
(11) Round, C. I.; Williams, C. D.; Duke, C. V. A. *Chem. Commun.* **1997**, 1849.
(12) Ko, Y. H.; Kim, S. J.; Kim, M. H.; Park, J. H.; Parise, J. B.; Uh, Y. S. *Microporous Mesoporous Mater.* **1999**, *30*, 213.
(13) Tusar, N. N.; Logar, N. Z.; Arcon, I.; Thibault-Starzyk, F.; Ristic, A.; Rajic, N.; Kaucic, V. *Chem. Mater.* **2003**, *15*, 4745.
(14) Rouquerol, F.; Rouquerol, J.; Sing, K. *Adsorption by Powders & Porous Solids*, 1st ed.; Academic Press: San Diego, 1999; p 378.

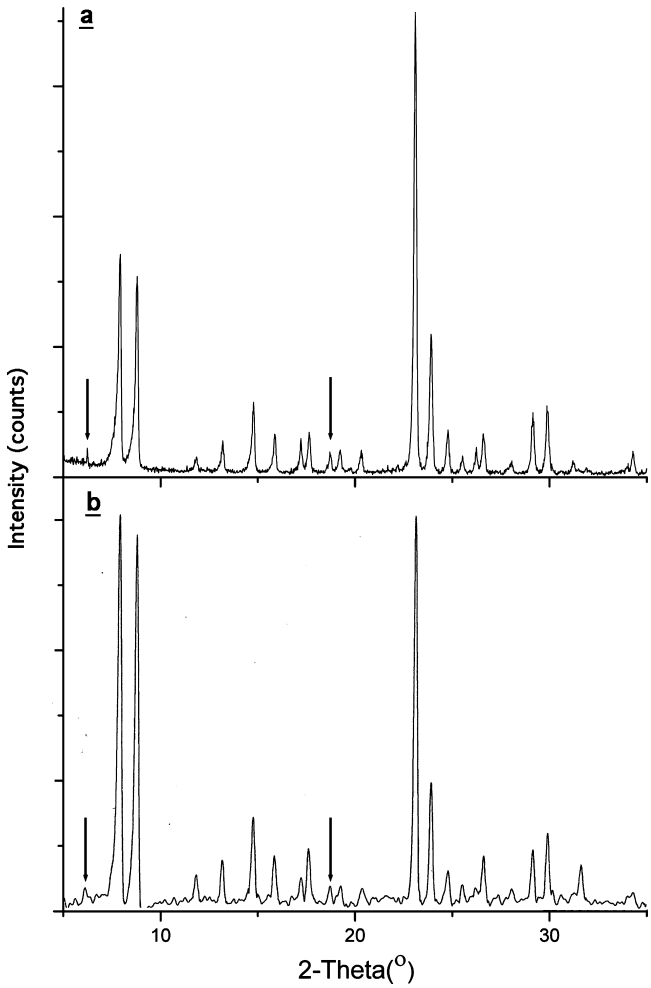

Figure 1. XRD pattern of 1 mol % manganese silicalite-2 calcined at (a) 500 °C and (b) 750 °C (arrows indicate the 110 and 330 reflections characteristic of the MEL structure).

reflections are observed at $2\theta = 23.1°$ for (501) and $2\theta = 23.9°$ for (303), which are seen in phase-pure ZSM-11 but not in mixed ZSM-11/ZSM-5 materials.[15,16] XRD analysis as a function of added manganese indicates that up to 2.5 mol % remains phase-pure ZSM-11. Above 2.5 mol %, biphasic materials were recovered that were not analyzed in detail. Imaging of the crystallites by TEM (Figure 2a) reveals well-defined planes with an interplanar spacing of ~9.7 Å, which corresponds to the (200) crystallographic planes. The material shows a sharp electron diffraction pattern (Figure 2b) that can be readily indexed to the ZSM-11 unit cell. An SEM image of the material containing 1 mol % Mn (Figure 3a) shows it to be composed of extremely well-formed crystallites of ~7 μm in length. In fact, the images show a clearly resolved arrangement of crystal faces (Figure 3b) that are compatible with $\bar{4}$ symmetry of the $I\bar{4}m2$ space group of ZSM-11. Interestingly, the manganese-containing materials exhibited larger, better-formed crystallites than did control samples containing no manganese made under the same conditions with the DDP template. A similar result has been reported previously for highly phase-pure ZSM-11, where the addition of an alkali-metal cation resulted in larger crystallite formation.[15] The unit cell parameters for each of the manganese silicalite-2 samples were refined in the tetragonal $I\bar{4}m2$ space group of ZSM-11 to obtain an accurate unit cell volume. A plot of the unit cell volume obtained from these refinements is shown in Figure 4. There is a linear increase in volume as a function of manganese loading, which is generally taken as indicative of metal ion substitution into the lattice, and while it does not quantify the amount of lattice incorporation per amount of added manganese, it does establish that a systematic and proportional incorporation is realized for each loading.

From a synthetic standpoint, an important question is, what percentage of the manganese available in the $Mn_{12}O_{12}(O_2CCH_3)_{16}$ cluster is being delivered to the silicalite? The cluster itself, which has been extensively studied as a single molecule magnet, is a mixed-valence ring structure containing eight Mn^{III} ions arranged in a circle with bridging acetate groups and a core of four Mn^{IV} ions bonded through oxo bridges.[5,17] While each cluster can potentially deliver 12 Mn atoms if all are incorporated, less incorporation would be expected if one oxidation state of the cluster were selectively incorporated. In the preparation of 2 mol % manganese silicalite-2, 1.14×10^{-4} mol of $Mn_{12}O_{12}(O_2CCH_3)_{16}$ is added to 0.068 mol of TEOS to achieve 0.020 mol of Mn atoms for every 1 mol of silicon. Elemental analysis of the calcined manganese silicalite-2 gave 1.98% Mn, which corresponds to 99.21% of the Mn provided by the cluster ultimately found in the silicalite product. The liquid remaining after the silicalite product was centrifuged, filtered, and analyzed. The amount of manganese remaining in the solution phase (i.e., not incorporated in the solid product) after synthesis proved to be negligible (<0.01 mmol). Because we detect no large-scale phase separation into manganese oxides within the detection limits of the XRD, it appears that the cluster is nearly quantitative in delivering all of its manganese, regardless of the initial oxidation state, to the silicalite though, as stated above, we cannot discriminate between framework and extra-framework speciation. Interestingly, attempts to synthesize manganese silicalite-1 by this approach using tetrapropylammonium hydroxide as the SDA were not successful, producing poor-quality materials with little insertion of the manganese. The reason for this is unknown, but it does suggest that specific interactions between the SDA and the transition-metal ion source may be important in the synthesis.

Oxidation State of the Mn. Analysis of the oxidation state for the calcined materials is provided by $L_{2,3}$-edge XANES. Figure 5 shows the XANES spectrum of a 1 mol % sample of manganese silicalite-2 calcined at 500, 650, and 750 °C for a period of 24 h under a dioxygen flow. Also shown, for purposes of assigning the oxidation state, are manganese oxide reference compounds in the II, III, IV, and mixed-valance II/III oxidation states. As indicated by the XANES spectra, calcination at 500 °C, which removes the organic

(15) Piccione, P. M.; Davis, M. E. *Microporous Mesoporous Mater.* **2001**, *49*, 163.
(16) Terasaki, O.; Ohsuna, T.; Sakuma, H.; Watanabe, D.; Nakagawa, Y.; Medrud, R. C. *Chem. Mater.* **1996**, *8*, 463.
(17) Sessoli, R.; Gatteschi, D.; Caneschi, A.; Novak, M. A. *Nature* **1993**, *365*, 141.

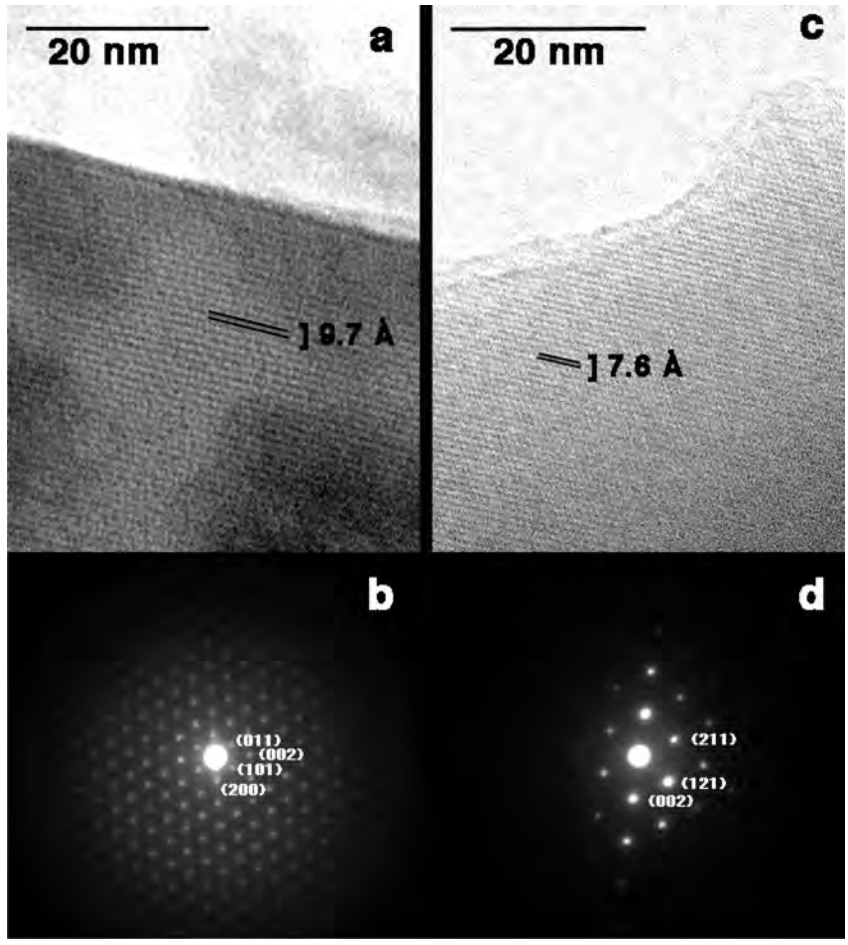

Figure 2. TEM of manganese silicalite-2 calcined at 500 °C: (a) image; (b) electron diffraction. TEM of manganese silicalite-2 calcined at 750 °C: (c) image; (d) electron diffraction

template, yields, within the detection limits of the XANES measurement, purely Mn^{II} sites in the lattice. These results suggest that, during the hydrothermal synthesis and initial calcinations, Mn^{III} and Mn^{IV} of the cluster get reduced and are incorporated into the silicalite channels as Mn^{II}. It should be noted, however, that manganese(II) acetate itself has been used in a previous high-pH synthesis of manganese silicalite-1 where high manganese loading was not achieved.[13] Likewise, in our initial attempts to make manganese silicalite-2, the use of simple Mn^{II} salts [i.e., $Mn(NO_3)_2$ and $MnCl_2$] and both manganese(II) and manganese(III) acetate complexes did not result in significant manganese incorporation. Clearly, the ability of the Mn_{12} cluster to deliver manganese to the lattice is unique and likely results from the formation of intermediate species stable at high pH and not simply through reduction to Mn^{II} or, more specifically, manganese(II) acetate.

Some structural information about the geometry of the manganese in the silicalite lattice can be inferred from the XANES spectra by a comparison with the controls. In particular, a comparison of the spectra of the MnO control, in which the manganese is in an octahedral environment, is quite similar at both the L_2 and L_3 edges with that of manganese(II) silicalite-2, suggesting that the geometries of the sites are the same. The absorption spectrum of Mn^{II} at the L_3 edge shows several sharp features, which are attributed to a combination of crystal-field effects with splitting due to multipole 2p−3d and 3d−3d interactions.[18] The intensity of these features is strongly dependent on the geometry and crystal-field strength around the ion. These resolved features for MnO are largely duplicated in manganese(II) silicalite-2, which is further suggestive of a similarity in the coordination environment. The low-energy peak at 634 eV, which is well resolved in MnO, appears as a shoulder in manganese(II) silicalite-2, which is consistent with the existence of a weaker ligand-field environment in this material. The XANES of Mn^{III} in silicalite-2 is virtually identical with that of the Mn_2O_3 reference in which Mn^{III} is in a distorted six-coordinate environment with two elongated Mn−O bonds. Taken together, the XANES spectra suggested that for both oxidation states the Mn is six-coordinate in the silicalite lattice. Because $Mn^{2+/3+}$ is replacing Si^{4+} in the silicalite, it will be 4-fold-coordinated by the lattice with the excess negative charge balanced, presumably, by a proton. Because the XANES spectra were collected under ambient conditions where hydration had the opportunity to occur, it is assumed that the vacant coordination sites are occupied by water molecules, which yield the distorted octahedral geometry.

(18) Cramer, S. P.; Degroot, F. M. F.; Ma, Y.; Chen, C. T.; Sette, F.; Kipke, C. A.; Eichhorn, D. M.; Chan, M. K.; Armstrong, W. H.; Libby, E.; Christou, G.; Brooker, S.; McKee, V.; Mullins, O. C.; Fuggle, J. C. *J. Am. Chem. Soc.* **1991**, *113*, 7937.

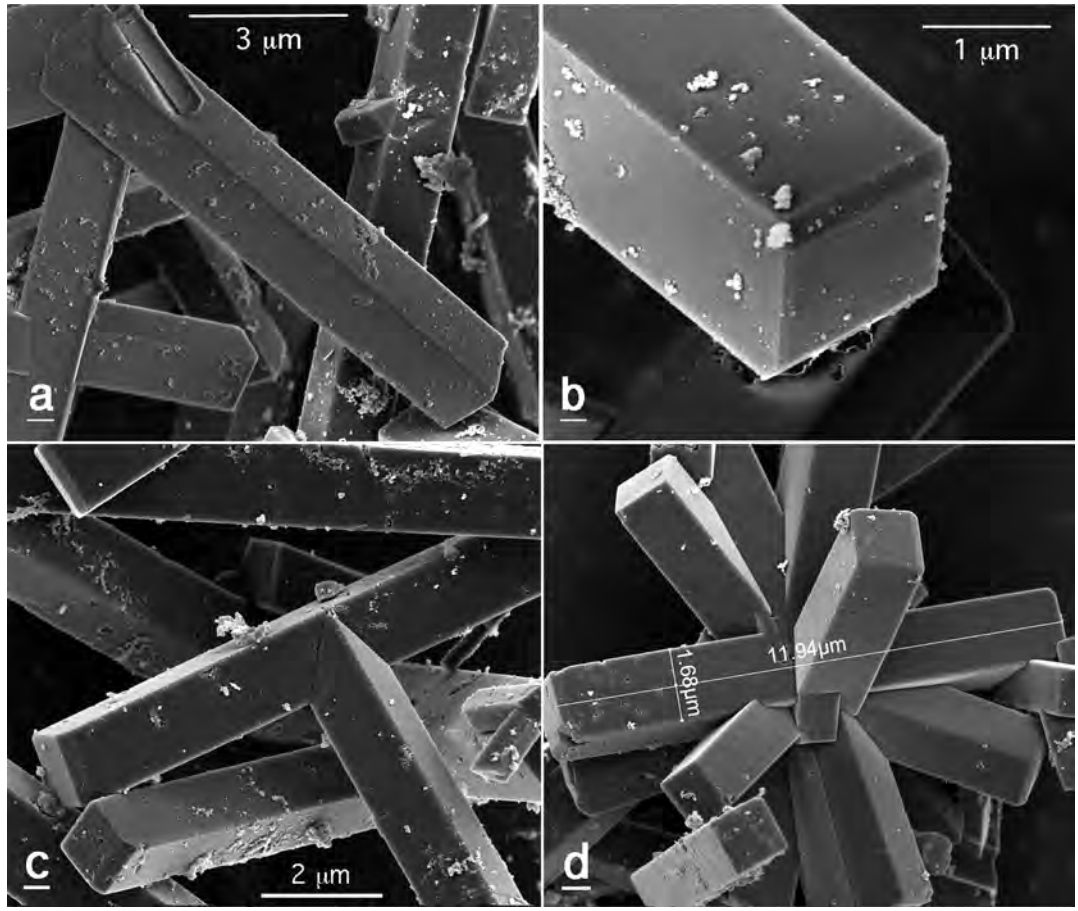

Figure 3. SEMs of manganese silicalite-2: (a) calcined at 500 °C showing representative crystallites; (b) the crystal faces that define the crystal habit; (c) calcined at 750 °C showing representative and (d) highly twinned crystallites.

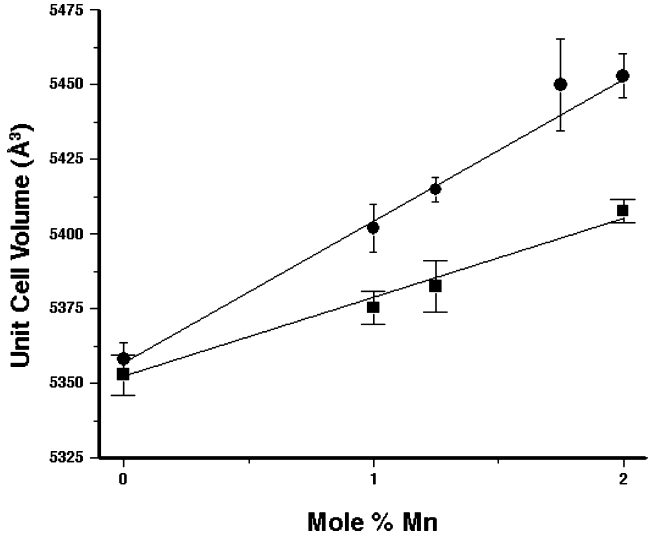

Figure 4. Plot of the unit cell volume as a function of Mn^{3+} (■) and Mn^{2+} (●) concentration.

This suggestion is supported by the presence of hydroxyls in the infrared spectrum.

Incorporation of Mn into the Lattice. As indicated by the XANES data, the Mn is in the II oxidation state at the end of the synthesis and after calcination, suggesting that somewhere during the process the Mn has been reduced from the III/IV states present in the Mn_{12} cluster. EPR spectra, collected in X band (Figure 6a), of the as-synthesized manganese silicalite-2 show a well-resolved hyperfine sextet characteristic of Mn^{II}, suggesting that either all or part of the Mn is reduced during the hydrothermal synthesis stage of the process. How $Mn^{III/IV}$ is reduced is unclear but probably involves oxidation of some of the organic species present in solution. Insights into Mn^{II} incorporation into the silicalite lattice can also be obtained from EPR spectroscopy. The EPR spectra of Mn^{II} ions randomly oriented in inorganic matrixes where axial symmetry has been imposed on the site are well understood. The outer transitions are not observed, and the spectra are characterized by a single $M_s = {}^1/_2 \leftrightarrow -{}^1/_2$ resonance.[19–23] As mentioned, the X-band spectrum of uncalcined manganese silicalite-2 (Figure 6a) shows a well-resolved hyperfine sextet from the $I = {}^5/_2$ nucleus with $g = 2.005$ and $A = 0.0087\ cm^{-1}$ corresponding to this transition. The position of the main resonance at a g value very close to 2 and the observation of well-resolved hyperfine coupling are consistent with a small zero-field splitting. Spectra collected at 5 K at Q band (Figure 6b) show further resolution of five of the six hyperfine lines into doublets. These lines

(19) Audi, A. A.; Sherwood, P. M. A. *Surf. Interface Anal.* **2002**, *33*, 274.
(20) Brouet, G.; Chen, X. H.; Lee, C. W.; Kevan, L. *J. Am. Chem. Soc.* **1992**, *114*, 3720.
(21) De Vos, D. E.; Weckhuysen, B. M.; Bein, T. *J. Am. Chem. Soc.* **1996**, *118*, 9615.
(22) White, L. K.; Szabo, A.; Carkner, P.; Chasteen, N. D. *J. Phys. Chem.* **1977**, *81*, 1420.
(23) Dewijn, H. W.; Vanbalde, Rf. *J. Chem. Phys.* **1967**, *46*, 1381.

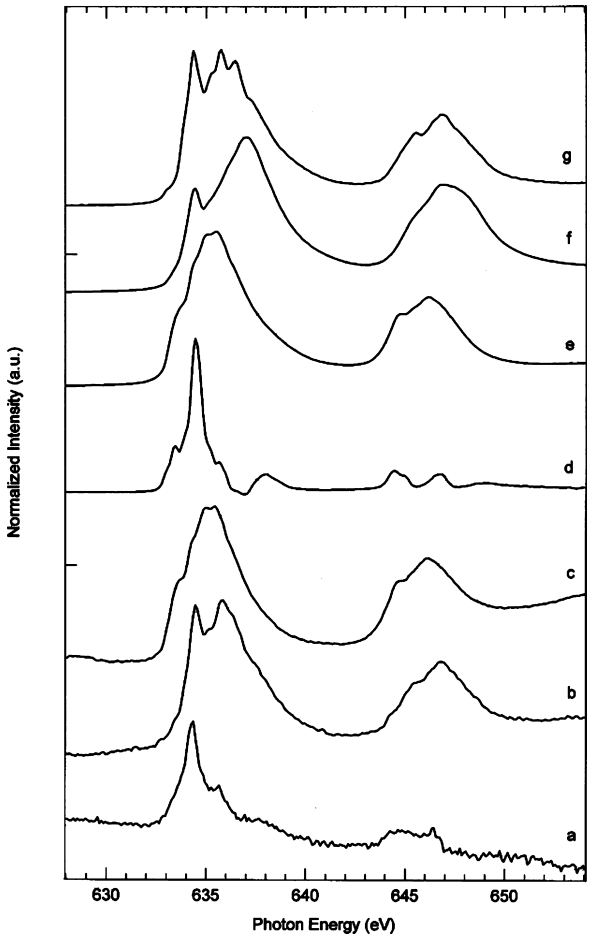

Figure 5. XANES spectra ($L_{2,3}$ Mn edge) of 1 mol % manganese silicalite-2 calcined at (a) 500 °C, (b) 650 °C, and (c) 750 °C and reference compounds (d) MnO, (e) Mn_2O_3, (f) MnO_2, and (g) Mn_3O_4.

have been observed previously and assigned to the formally nonallowed $\Delta m_I = \pm 1$ transitions of the central $M_s = {}^1/_2 \leftrightarrow -{}^1/_2$ resonance.[23] The relative intensities of the allowed and forbidden lines are proportional to $(D/H_0)^2$ where D is the zero-field splitting and H_0 the magnetic field. Integration of the Q-band spectra and measurement of the intensities of allowed and nonallowed transitions yield a zero-field splitting of 0.014 ± 0.004 cm^{-1}.[21,24] This small zero-field splitting indicates that the Mn^{II} ions in the as-synthesized silicalite-2 are largely octahedral with only small axial distortion. Notably, both the magnitude of the hyperfine coupling and the zero-field splitting are very close to those observed by De Vos et al. for Mn^{II} ions exchanged into the pores of NaA zeolites.[21] Because the system dehydrates during heating at the calcination temperature (500 °C), there is complete loss of the hyperfine structure (Figure 7), which is consistent with the large increase in the zero-field splitting that would accompany the loss of octahedral symmetry when the ion is inserted into the lattice. Notably, loss of the hyperfine structure in Figure 6 could also be explained by spin−spin interactions due to agglomeration of the manganese, that would necessitate severe demetalation of the lattice, which is inconsistent with the crystallographic data. All in all, this

(24) Shaffer, J. S.; Farach, H. A.; Poole, C. P. *Phys. Rev. B* **1976**, *13*, 1869.

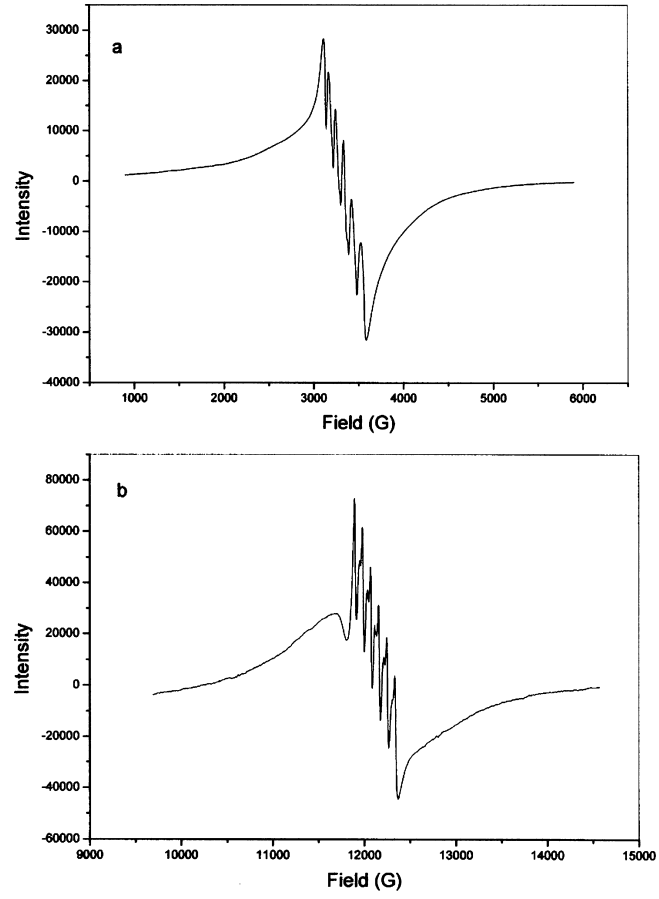

Figure 6. EPR spectra of as-synthesized (uncalcined) 0.5 mol % manganese silcialite-2 at room temperature collected in (a) X band and (b) Q band.

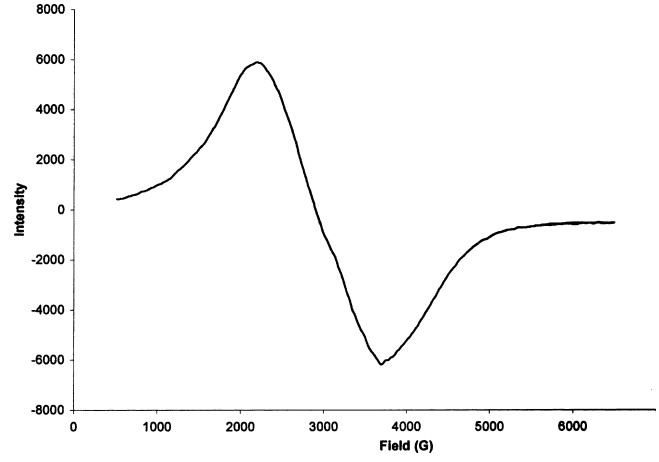

Figure 7. X-band EPR spectrum of 0.5 mol % manganese silicalite-2 calcined for 24 h at 500 °C under dioxygen.

suggests that, in the as-synthesized manganese silicalite-2, the Mn ions are not strongly incorporated into the silicalite lattice and that actual insertion into the framework occurs with calcination. This suggestion is supported by changes in the unit cell volume as a function of the processing temperature. Clearly, substitution of the metal ion into the silicalite lattice takes place in several stages, with the hydrothermal synthesis delivering the metal ion into the pores. At this stage, the coordination sphere is hydrated and, perhaps, loosely associated with the lattice, as suggested by the small zero-field splitting in the EPR spectrum. Calcination

at a temperature that removes the organic template also results in insertion of the Mn^{II} ion into the lattice.

Above that temperature, at 650 °C the Mn is further oxidized and a mixture of Mn^{II} and Mn^{III} appears to be present. The mixed valency of the 650 °C calcined manganese silicalite-2 is supported by the similarity of its XANES with that of the mixed-valence Mn_3O_4 reference standard (Figure 5g). Materials calcined at 750 °C undergo relatively complete conversion to Mn^{III}, as evidenced by the XANES spectrum (Figure 5b). These results are generally consistent with those reported for manganese silicalite-1 by Tusar et al., who confirmed the presence of Mn^{III} along with some unoxidized Mn^{II} upon 550 °C oxidation.[13] However, in manganese silicalite-2, the oxidation to Mn^{III} appears to occur at higher temperatures, well separated from the initial calcination temperature of Mn^{III}. From the standpoint of use in applications such as catalysis, this is advantageous because it suggests that relatively pure oxidation state manganese(II) and manganese(III) silicalite-2 can be made.

Gas physisorption of materials oxidized at 750 °C to Mn^{III} show retention of the type I isotherm and the H4 hysteresis loop.[9] The BET surface area is 298 m^2/g, and the average pore diameter is 0.49 nm. The X-ray analysis indicates that it is still phase-pure ZSM-11 of apparently good crystallinity (Figure 1b). The diffraction peaks are slightly broader than those of the Mn^{II} materials, indicating that there may be some slight degradation due to thermal processing. TEM (Figure 2c) of the crystallites resolves well-defined planes with an interplanar spacing of ~7.5 Å, which corresponds to the (211) crystallographic planes. The material shows a diffraction pattern (Figure 2d) that is indexed to the ZSM-11 unit cell. Imaging of the crystallite by SEM (Figure 3c) shows them to be very well-formed rods, on the order of 7−15 μm long and 1.68 μm square, which are identical in habit with the materials calcined at 500 °C. Interestingly, the SEM images of this sample also showed a number of structures composed of highly twinned or even more complex intergrown arrangements of crystallites (Figure 3d). While the materials are still silicalite-2 after high-temperature oxidation, an important question is whether Mn^{II} is still present in the lattice. The unit cell volume, obtained from the refined XRD pattern as a function of manganese loading, is shown in Figure 4. For a given concentration of manganese, the unit cell volume would be expected to decrease when Mn^{II} is oxidized to Mn^{III} due to a change in the ionic radius from 0.80 to 0.66 Å.[25] This is observed at each of the manganese loadings. The general trend, however, is that the unit cell volume increases as a function of the Mn^{III} concentration, consistent with the systematic incorporation into the lattice.

In conclusion, we have established that the choice of molecular precursors can have an important impact on the synthesis of framework-substituted silicalite under conditions of high pH. By use of $Mn_{12}O_{12}(O_2CCH_3)_{16}$ as a Mn source, manganese silicalite-2 was synthesized at high pH and with loadings of up to 2.5 mol %. Studies of the effects of the calcination temperature of this system found that both manganese(II) and manganese(III) silicalite-2 can be prepared by the choice of the calcination temperature. This provides a pathway to two distinct substituted silicalites, whose catalytic activities are likely to be different.

Acknowledgment. Funding was provided by the Air Force Office of Scientific Research through MURI 1606U81. This work was partially supported by the Office of Basic Energy Sciences, Division of Materials Science, under the auspices of the U.S. Department of Energy by the University of California, Lawrence Livermore National Laboratory, under Contract W-7405-Eng-48. The work conducted at the Advanced Light Source is supported by the Director, Office of Science, Office of Basic Energy Sciences, Materials Sciences Division, of the U.S. Department of Energy under Contract DE-AC03-76SF00098 at Lawrence Berkeley National Laboratory.

IC800366J

(25) *Handbook of Chemistry and Physics*, 56th ed.; CRC Press: Boca Raton, FL, 1975.